Static and Dynamic Fluorescence from α,ω-Di(1-pyrenyl)alkanes in Polyethylene Films. Control of Probe Conformations and Information about Microstructure of the Media

Oscar E. Zimerman and Richard G. Weiss*

Department of Chemistry, Georgetown University, Washington, D.C. 20057-1227

Received: August 25, 1997; In Final Form: February 27, 1998

Static and dynamic fluorescence from four α,ω-bis(1-pyrenyl)alkanes (P*n*P, where *n*, the number of carbons atoms in the alkane chain, is 3, 5, 7, and 12) has been examined in two polyethylene films of 31% (LDPE) and 71% (HDPE) crystallinity. Fluorescence decays of four P*n*P at $\sim 10^{-5}$ M *bulk* concentrations, including that of P7P which is monoexponential in hexane, are biexponential in the films ($\tau_1 \sim 200$ ns; $\tau_2 \sim 40-60$ ns). Since 1-ethylpyrene, a monolumophoric model for the P*n*P, provides monoexponential decays ($\tau \sim 200$ ns) in both hexane and the films, the P*n*P interchromophoric interactions in the PE films are *intra*molecular. Dynamic excimer formation is evident only for P3P in LDPE; static excimeric emissions are observed for P3P in LDPE and HDPE and for P5P in LDPE. Especially in interfacial sites of the PE films, the lumophoric groups of the P*n*P appear to adopt specific conformations that are not detectable in "normal" isotropic liquid or glassy media. A model to account for these results that involves these conformations and the lateral surfaces of PE microcrystallites is presented.

Introduction

At room temperature, polymers such as polyethylene (PE) consist of ordered (crystalline) domains and amorphous parts whose chains are disordered and resemble a static picture of the liquid state.[1] Chain-folded lamellae[2] with thicknesses of typically 100−200 Å and widths in the micrometer range were discovered when a single crystal of PE became available. Electron diffraction shows that the long axes of the chains are perpendicular (or nearly so) to the broad surface of a lamella.[3−5] Immediately next to the lateral faces of the crystallites are parallel polymethylenic segments, arranged orthogonally to the broad surface of a lamella, that constitute the interfacial "regions".[3−6] Electron micrographs of PE show the presence of a superstructure of microcrystals, called spherulites, consisting of chain-folded lamellae of narrow width (ribbons) projected radially and extending over micrometers in a sea of amorphous chains. Thus, the lamellar chains are normal, on average, to a radius. Spiral lamellae, dendrites, and an overgrowth of extended-chain fibril called "shish kebob", can also be present.[3,4] However, the supramolecular structure has little, if any, direct influence on many bulk properties of PE.[5]

The interstitial spaces between chains in the noncrystalline regions are commonly referred to as "free volume" (or "hole" free volume).[7,8] It is continuously redistributed by thermal fluctuations in the absence of guest molecules. In their presence, the redistribution of free volume controls both diffusion and the preferred guest sites.[7,8] Diffusion of most dopant molecules in polymers occurs within the amorphous and interfacial parts. Only very small species, like helium, enter the crystalline part.[9]

Upon stretching, the spherulitic organization is transformed into partially oriented, separated microcrystallites; additionally, some of the methylenic chains in the amorphous regions become partially oriented in the direction of the applied stress.[10] This alignment is commonly used to orient dopant molecules in the films,[11] and to direct their chemical reactions and alter their diffusion.[12] Film stretching has also yielded valuable information on the structure of polymer crystals and on the crystallization of polyolefins adsorbed to them.[13] Fluorescence, pulse radiolysis,[14] and polarized absorption spectroscopy[15] are among the techniques that have been applied to study the static and dynamic properties of guest molecules in PE films. For example, the rates of diffusion of *N*,*N*-dialkylanilines (DAA)[16] and the concentration dependence of pyrene on excimer formation in native PE films have been determined from fluorescence data.

Despite the enormous effort to understand PE, many questions concerning how it interacts with guest molecules are unanswered. Among these are the following: (1) What is the distribution of guest molecules between amorphous and interfacial sites? (2) Do guest molecules prefer to aggregate at one type of site? (3) How do the "walls"[10c,17] of PE guest sites affect the conformations and dynamics of alkyl chains?

To address these and other questions, we examine here the static and dynamic spectroscopic properties of four, α,ω-di(1-pyrenyl)alkanes (P*n*P where *n*, the number of methylene groups, is 3, 5, 7, or 12) and a "model" compound, 1-ethylpyrene (EtPy), in two polyethylene films of differing degrees of crystallinity, and compare the results with those in the isotropic hydrocarbon solvent hexane. We attempt to relate the fluorescence properties of the pyrenyl guests to the natures of the sites they occupy in polyethylene to test further and refine the models developed previously.[12,16,18,19]

At high bulk concentrations ($\sim 10^{-2}$ M) of pyrene, excimer emission is observable in PE due to ground-state molecular aggregates near or at the excimer configuration.[20] For fluorescence decay histograms of pyrene[21] (or EtPy)[22] in poly(methyl methacrylate) (PMMA), either biexponential decays or more complex decays were observed.

In isotropic media, nearly all P*n*P ($n = 2-16$, 22) provide emission from an intramolecular, dynamically formed excimer.[23] The ratio of excimer to monomer fluorescence intensity varies nonsystematically with *n*; a lack of excimer emission from P7P has been attributed to conformational barriers along the poly-

S1089-5639(97)02758-8 CCC: $15.00
Published on Web 04/23/1998

methylene chain.[24] From studies of pressure on the luminescence of P3P in various solvents, it was concluded that intramolecular excimer (IE) formation is strongly dependent on solvent viscosity, but almost independent of solvent polarity.[25]

Despite the extensive investigations of time-resolved fluorescence from P3P in isotropic solvents, no consensus concerning the mechanism for formation of its excimer has emerged.[26,27] P10P is the only other P*n*P homologue for which extensive dynamic measurements appear to have been reported in isotropic solvents.[26a] Fluorescence decay data indicate that P3P barely penetrates both anionic and cationic surfactant micelles, but freezing and thawing of the micellar solutions accelerates solubilization.[28] The properties of IE formation in multilayer dispersions and sonicated vesicles show that P3P molecules have a marked effect on the disposition of nearby host lipids.[29] Static and dynamic aspects of IE formation of P*n*P (n = 3, 10, 13, 22) in a cholesteric phase and in the nematic and smectic phases of *trans,trans*-4-*n*-butylbicyclohexane-4-carbonitrile have been compared with data from the corresponding isotropic phases.[30b] The activation energies for excited monomer quenching indicate that the influence of mesophase order on P*n*P chain bending depends strongly on *n*; there is no direct correlation between the activation parameters in the isotropic and meso phases.

These examples demonstrate the utility of P*n*P homologues to assess the nature of their immediate environments. Here, we use static and dynamic fluorescence from P*n*P homologues to probe the limitations to translational and conformational mobility imposed by guest sites of PE. Our data demonstrate that P3P and the other P*n*P investigated behave very differently in PE films than they do even in frozen hydrocarbon matrixes; *the polyethylene microenvironments experienced by the PnP are not analogous to those in a very viscous or glassy hydrocarbon solution*.

Experimental Section

Reagents. PE films are designated LDPE **(**blown Type NA-203 from Polyolefinas; M_w = 510 000 according to the manufacturer; 140 μm thick, 31% crystallinity according to differential scanning calorimetry (DSC[18])) and HDPE (Type ES-300 from Polialden Petroquimica; 20 μm thick, 71% crystallinity (from DSC[18]). Density and film thickness (calculated from IR interference fringes) were determined previously.[18]

1,3-Di(1-pyrenyl)propane (P3P) (mp 148−149 °C (lit.[30b] mp 148−150 °C)) and 1-ethylpyrene (mp 95−96 °C (lit.[31] mp 94−95 °C)) were obtained from Molecular Probes and used as received. P5P (mp 184−186 °C (lit.[23] mp 188−189 °C)), P7P (mp 136−138 °C (lit.[30b] mp 137−139.5 °C), and P12P (mp 129−130 °C (lit.[30c] mp 129.5−130.5 °C)) were available from previous work.[30] From HPLC analyses performed on a Waters chromatograph (UV detector; 254 nm), P5P, P7P, and P12P were >99% pure (Alltech Econosphere 5 μm, 250 mm length × 4.6 mm i.d. silica column; *n*-hexane as eluant) and EtPy and P3P were >99% and ∼99% pure, respectively (Waters Symmetry C_{18} 150 mm length × 3.9 mm i.d. column; 2/1 (v/v) acetonitrile/water as eluant). Methanol (Mallinckrodt UltimAR 99.9%), acetonitrile (Fisher Scientific, HPLC grade), *n*-hexane (EM Science, spectrophotometric grade), *n*-heptane (EM Science, spectrophotometric grade; chromatographed over Al_2O_3; >99.9% by gas chromatographic analysis), and chloroform (Mallinckrodt, spectrophotometric grade) were used as received. *n*-Heneicosane (C_{21}) (mp 40−41 °C (lit.[32] mp 40.14 °C)) was obtained from Humphrey and recrystallized three times from 95/5 acetone/hexane.

Preparation of P*n*P and EtPy Samples in Hexane or Heptane. Aliquots of 10^{-5} M EtPy or 5×10^{-6} M P*n*P in a hydrocarbon solvent were flame-sealed in Kimax flattened glass capillaries (8 mm (i.d.) × 0.4 mm (i.d.) × 40 mm, Vitro Dynamics) after being degassed (four freeze−pump−thaw cycles at $<10^{-5}$ Torr).

Preparation of P*n*P and EtPy-Doped PE Films. Before being used, films of PE were immersed overnight in chloroform to remove antioxidants, washed with methanol, and dried in a stream of nitrogen. Typically, strips of "clean" PE (∼1.5 × 0.5 cm) were immersed overnight in a ∼0.01 M chloroform solution of P*n*P or EtPy. The films were rinsed thoroughly with methanol to remove any surface P*n*P and dried with a stream of nitrogen; this lead to $\sim 10^{-5}$ M concentrations of P*n*P or EtPy in the films. The precise concentrations were calculated using Beer's law and the average absorbance from three UV spectra recorded at different positions of each film and assuming ϵ_{343} 79 600 M^{-1} cm^{-1} for P*n*P and 39 800 M^{-1} cm^{-1} for EtPy.[33] Then, films were placed into Kimax flattened glass capillaries that were degassed at $<10^{-5}$ Torr and flame-sealed.

Doped films (∼1.5 × 0.5 cm) were cold stretched by hand to ∼4 times their initial lengths, folded upon themselves three or four times, flattened to make an area ∼4 × 7 mm, placed in capillaries, and sealed as above.

Preparation of P7P in C_{21}. A small amount of P7P mixed with C_{21} was melted (∼50 °C) and gently shaken in a vial. The precise concentration was determined by UV absorption in the isotropic phase. An aliquot of appropriate composition was transferred to a Kimax flattened glass capillary that was flame-sealed after the sample was degassed in the isotropic phase by four freeze−pump−thaw cycles at $<10^{-5}$ Torr.

Instrumentation. All data were collected at ambient temperatures. UV/visible absorption spectra were recorded on a Perkin-Elmer Lambda-6 spectrophotometer. Films were mounted in the air on an aluminum holder, and an undoped clean film was used as reference. Excitation (corrected for detector response) and emission spectra (uncorrected) were obtained on a Spex Fluorolog 111 spectrofluorometer (linked to a PC) with a 150-W high-pressure xenon lamp and 0.25-mm slits on both the excitation and the emission monochromators. Fluorescence rise and decay histograms were obtained with an Edinburgh Analytical Instruments model FL900 single-photon-counting system using H_2 as the lamp gas. Samples in Kimax capillaries were aligned at 45° to the incident radiation, and emission was detected at a right angle from the back face of the film. An "instrument response function" was determined using Ludox as a scatterer, and no polarizer filters were used. Typically, the half-width duration of the pulses was ∼2 ns and the pulse rate was ≤40 kHz. In all cases, at least 10^4 counts were collected in the peak channel.[34] Data were collected in 1023 channels (1.009 ns/channel), and analyses were based on 1003 channels.

Molecular Modeling. Calculations employed the AM1 semiempirical self-consistent field (SCF) method in the HyperChem release 5.01 for Windows95 package. Default parameters were used throughout.

Fluorescence Decay Data Treatment. Deconvolution was performed by nonlinear least-squares routines, minimizing χ^2 with software supplied by Edinburgh. A range from before time 0 to at least two decades of decay from the peak channel were included in analyses. In almost all cases, a small "scatter" peak of very short duration was present in the decay profiles as a result of the poor optical quality of the flattened capillary surfaces; the apparent decay constants (nonsystematic) associated with the scatter are not reported. Goodness of fit was assessed from plots of residuals. Initially, monoexponential fits

were attempted. χ^2 values of <1.2 were deemed acceptable if no systematic deviation from zero in the residual plot was apparent. If unacceptable for either reason, two exponential terms, and so on, were used until satisfactory fits were achieved. Data were analyzed using either *exponential* or *global analysis*[35] methods. The exponential method was used when a single wavelength of emission and excitation was employed or no correlations were made among the decays. In addition, *distribution analyses*[36] of several of the same data sets were conducted. Distribution analyses were performed by the iterative reconvolution method[36b] employing up to 50 lifetimes using the software package supplied by Edinburgh.

Time-resolved emission spectra (TRES) using λ_{ex} 343 nm[37] were constructed from decay curves recorded at 5-nm increments of λ_{em}. Each set of decays was "sliced" at a time window following the excitation pulse to provide a TRES.

Results

Steady-State Fluorescence Measurements. No fluorescence from LDPE or HDPE could be detected when "clean," undoped films were irradiated in the region used to excite pyrenyl molecules.

n-Hexane solutions of $\sim 10^{-5}$ M P*n*P ($n \geq 3$) at room temperature exhibit a structured monomer emission at 360−400 nm and/or a broad, structureless intramolecular excimer band with a maximum near 500 nm. They are essentially the same as those reported for the P*n*P in methylcyclohexane at room temperature.[23] Emission spectra of all of the P*n*P and EtPy in both isotropic solvents and for the P*n*P with $n = 5$, 7, or 12 and EtPy in the two PE films are independent of λ_{ex}. Peak widths and shapes of monomer emissions from P5P, P7P, P12P, and EtPy in the PE films and in hydrocarbon solvents are comparable to those in the hydrocarbon solvents, but the former are red-shifted by ~2−3 nm, and the spectrum of P5P in LDPE, especially, is broadened in the longer wavelength portion.

It is not possible with the data at hand to determine *definitively* whether emission from excited-state complexes is the source of the slightly greater *relative* intensities at >400 nm from P5P in LDPE and from EtPy, P7P, and P12P in both PE films (than observed in hexane). However, the long wavelength tails at >450 nm do *not* appear to be due to emissions from complexes. The emission spectra, in combination with dynamic fluorescence intensity measurements (vide infra), demonstrate that there is some form of interlumophoric interactions present. Its nature is considered in the Discussion section.

Emission spectra from P3P in both PE films are much more complex than those in the hydrocarbon solvents. The shape of the monomer portion in LDPE is very dependent on λ_{ex}, but that in HDPE is not. The positions of the monomer emission bands from P3P at ~374 nm in the films and in hexane are the same (±1 nm). Each spectrum contains longer wavelength emissions that are typical of excimers.

Peak positions of the corresponding excitation spectra of EtPy and the P*n*P with $n = 5$, 7, and 12 are independent of λ_{em} and are red-shifted by 2−3 nm with respect to those in hexane, also. The excitation spectra of P5P in LDPE and of P12P in both films are broader when λ_{em} is 470 nm than when it is 343 nm. Unlike its emission spectra, the excitation spectra of P3P in PE are red-shifted with respect to those in hexane by 2−4 nm. In HDPE, the excitation spectra of P3P also broaden as λ_{em} is increased.

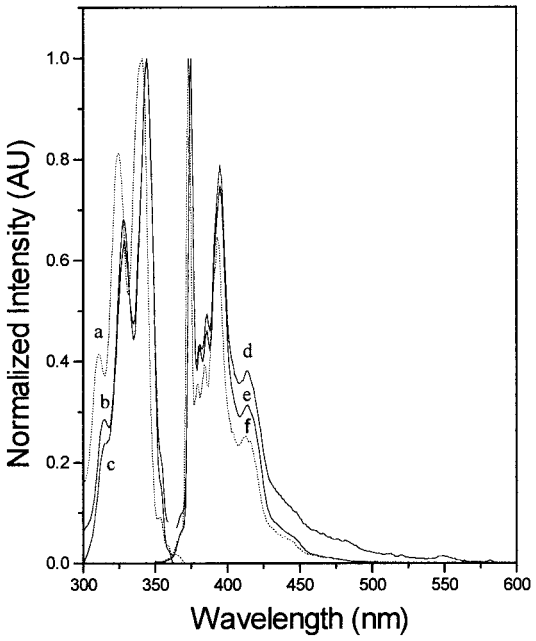

Figure 1. Normalized excitation (a−c) and emission (d−f) spectra of (≈10^{-5} M) 1-ethylpyrene in *n*-hexane (a, λ_{em} 375 nm; f, λ_{ex} 340 nm), HDPE (b, λ_{em} 373 nm; e, λ_{ex} 344 nm), and LDPE (c, λ_{em} 373 nm; d, λ_{ex} 344 nm).

TABLE 1: I_1/I_2 and I_1/I_3 Emission Intensity Ratios for EtPy, P3P, P5P, P7P, and P12P in *n*-Hexane, LDPE, and HDPE

	n-hexane		LDPE		HDPE	
probe	I_1/I_2	I_1/I_3	I_1/I_2	I_1/I_3	I_1/I_2	I_1/I_3
EtPy	1.56	3.97	1.27	2.62	1.33	3.18
P3P	1.21				1.14	2.53
P5P	1.32		1.04	1.69	0.96	2.25
P7P	1.56	4.10	1.45	3.88	1.54	4.05
P12P	1.11	3.97	1.07	2.35	1.15	2.79

Figure 1 shows normalized emission and excitation spectra of EtPy. Vibronic bands at 373 (I_1), 393 (I_2), and 413 nm (I_3) are present in both PE films. The ratios of I_1/I_2 *height* intensities for EtPy, P7P, and P12P (but not P5P), are slightly higher in HDPE than in LDPE (Table 1). Under the best of circumstances, these ratios are a weighted average of values from the different environments experienced by lumophores. Interestingly, I_1/I_2 and I_1/I_3 are less dependent upon the medium for P7P than for EtPy, a molecule that does not suffer chromophore−chromophore interactions under the conditions of our experiments.[23]

Like the emission spectra, excitation spectra of EtPy in the two PE films are virtually superimposable, but slightly narrower and 3 nm red-shifted (due to the greater polarizability of PE[38]) than those in *n*-hexane: compare for instance, the typical value of $\eta_D = 1.54$ for HDPE and $\eta_D = 1.52$ for LDPE[39] with $\eta_D = 1.37$ for *n*-hexane.[40] A *bulk* property like index of refraction is an even worse descriptor than the fluorescence intensity ratios of microenvironments in nonhomogeneous media like PE. Whereas peak intensitiy ratios relate only to the amorphous and interfacial parts of PE, a bulk property like index of refraction pertains as well to the crystalline part, where no EtPy or P*n*P molecules reside. Additionally, the frequency of more polarizable alkenyl groups in LDPE is twice as high as in HDPE.[18] For this reason, the values of η_D should be used to interpret our data only *qualitatively*: the polarizing power of PE is greater than that of hexane; the differences between the values for LDPE and HDPE are inconsequential with respect to our applications and the absolute values for *our* films have not been measured.

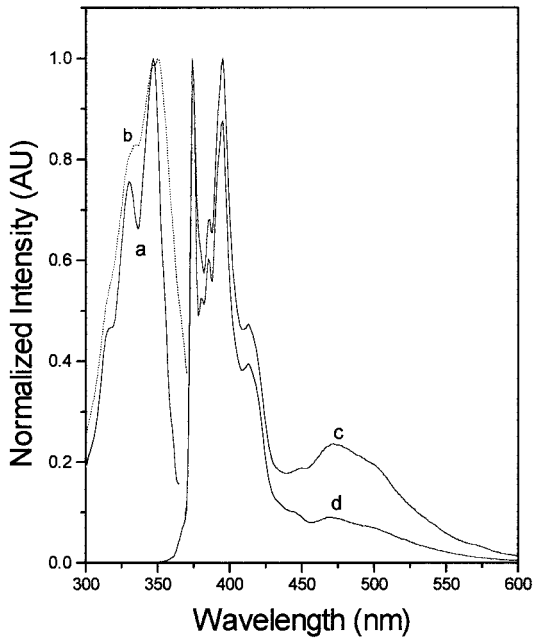

Figure 2. Normalized excitation (a, λ_{em} 374 nm; b, λ_{em} 471 nm) and emission (c, λ_{ex} 358 nm; d, λ_{ex} 343 nm) spectra of $\approx 5 \times 10^{-6}$ M P3P in HDPE.

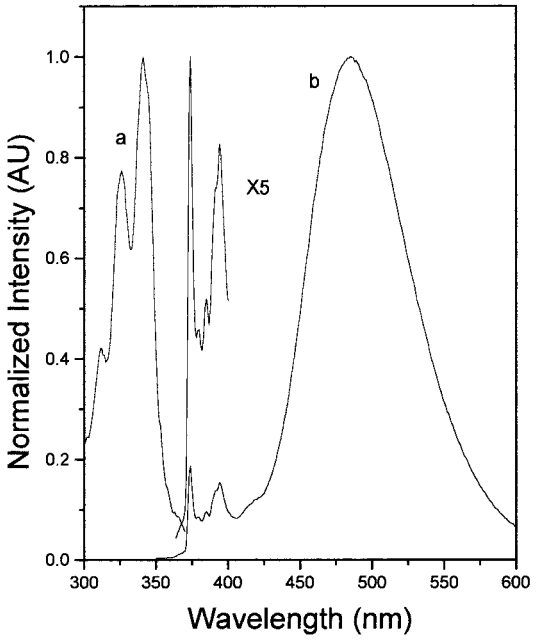

Figure 3. Normalized excitation (a, λ_{em} 373 nm), and emission (b, λ_{ex} 343 m) spectra of $\approx 5 \times 10^{-6}$ M P3P in *n*-hexane.

However, the values do suggest that molecules residing near well-ordered, parallel polymethylene chains (i.e., at the interfacial region) are subject to a greater polarization than those within less-ordered, more randomly oriented chains (i.e., in the amorphous region). The magnitude of spectral band shifts and the half-widths of individual bands may depend on the fraction of fluorescing pyrenyl groups in each environment.

Figure 2 contains normalized excitation and emission spectra of P3P in HDPE. The monomer portion of the emission with λ_{ex} 343 nm is like that of EtPy, or of P3P in *n*-hexane. The broadness of excitation spectrum b is indicative of the presence of ground-state species different from those responsible for (a). The emission spectrum also changes with excitation wavelength: more emission is produced in the excimer-rich region when λ_{ex} is 358 nm than when it is 343 nm. The wavelength dependence is not due to *inter*molecular interactions since the shapes of the spectra of EtPy at a bulk concentration of $\sim 1 \times 10^{-5}$ M (that is equal to the P*n*P pyrenyl concentrations) are independent of λ_{em} or λ_{ex} (Figure 1). More importantly, the fluorescence decay of EtPy is *monoexponential* (vide infra). In *n*-hexane, the intramolecular excimer band of P3P (from dynamically formed complexes[23]) is dominant at all wavelengths of excitation and the excitation spectrum is virtually indistinguishable from that of EtPy (Figure 3).

These results are consistent with previous observations that the absorption spectra of 1-methylpyrene and P*n*P (with $n \geq 3$) are the same in methylcyclohexane.[23] At −110 °C, where dynamic conformational motions are slowed, as they are in the amorphous parts of PE at room temperature, hydrocarbon solutions of P*n*P provide only monomer emissions whose appearance and lifetimes are like those of 1-methylpyrene.[23]

In HDPE, excitation and emission spectra of P5P, P7P, and P12P (Figures 4−6) are similar to those of EtPy (Figure 1). The monomer portions of the emission spectra of these P*n*P are virtually identical to those in LDPE or *n*-hexane. In addition, the excitation and emission spectra of P7P and P12P are virtually independent of the PE type. Based upon dynamic fluorescence measurements (vide infra), the very weak tails in the emission spectra that extend from ≈450 nm to >500 nm are *not* due to

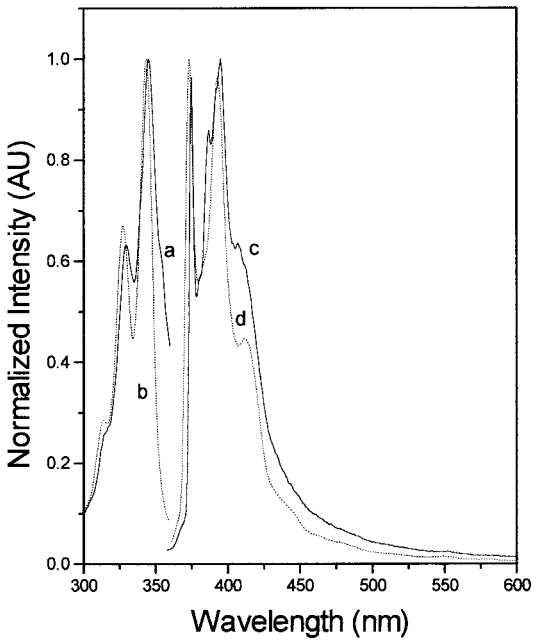

Figure 4. Normalized excitation (a, b) and emission (c, d) spectra of $\approx 5 \times 10^{-6}$ M P5P in LDPE (a, λ_{em} 373 nm; c, λ_{ex} 343 nm) and HDPE (b, λ_{em} 373 nm; d, λ_{ex} 344 nm).

molecules that emit from excimer-like conformations. In these and several of the other emission spectra, "bumps" along the red-edge tail are instrumental artifacts.

The emission spectrum of P5P in LDPE (Figure 4c) is dominated by monomer but exhibits an intense tail, consistent with the presence of some molecules emitting from an excimer-like conformation. The corresponding excitation spectrum indicates that some (if not all) of the excess red-shifted emission arises, again, from direct excitation of molecules in conformations that allow very strong interchromophoric interactions. Evidence for similar species is absent in the excitation and emission spectra of P5P in HDPE. In fact, the highest energy emission band of P5P in LDPE (Figure 4c) is at a slightly longer wavelength than that in HDPE (Figure 4d). The difference is outside the limits of instrumental resolution and, as explained

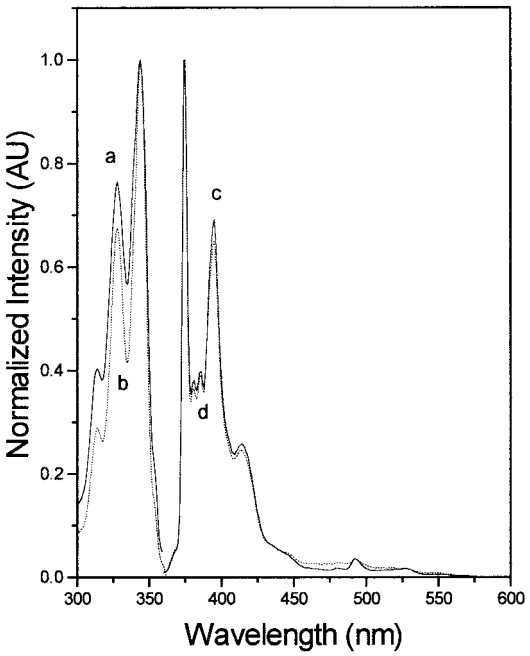

Figure 5. Normalized excitation (a, b) and emission (c, d) spectra of $\approx 5 \times 10^{-6}$ M P7P in LDPE (a, λ_{em} 374 nm; c, λ_{ex} 344 nm) and HDPE (b, λ_{em} 373 nm; d, λ_{ex} 340 nm).

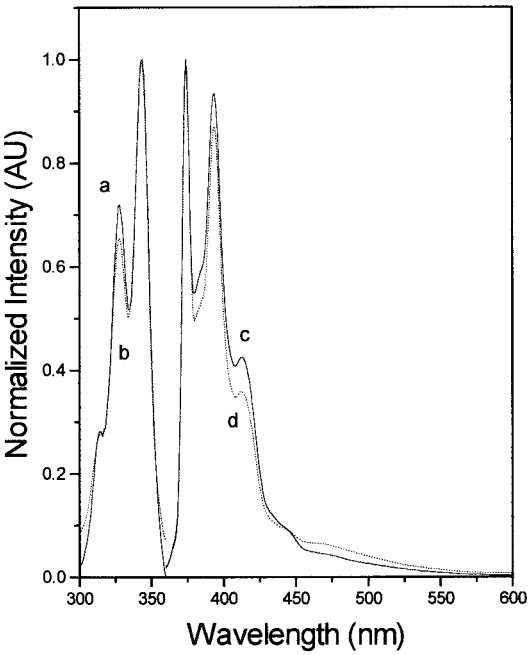

Figure 6. Normalized excitation (a, b) and emission (c, d) spectra of $\approx 5 \times 10^{-6}$ M P12P in LDPE (a, λ_{em} 374 nm; c, λ_{ex} 343 nm) and HDPE (b, λ_{em} 374 nm; d, λ_{ex} 343 nm).

above, cannot be associated directly with *bulk* electronic factors, like polarizability (vide ante).

The excitation and emission spectra of P3P in LDPE (Figure 7) are dependent on λ_{em} and λ_{ex}, respectively. For instance, the emission spectrum from λ_{ex} 348 nm is broad with a small, sharp peak at 373 nm but that from λ_{ex} 354 nm is even broader and lacks the feature at 373 nm. The shape of the emission spectrum is very different from that in HDPE and *n*-hexane. The excitation spectrum monitored at 485 nm is broader, red-shifted, and less well-defined than those from λ_{em} 374 or 404 nm. These spectra indicate the presence of a significant population of P3P molecules in ground-state conformations that

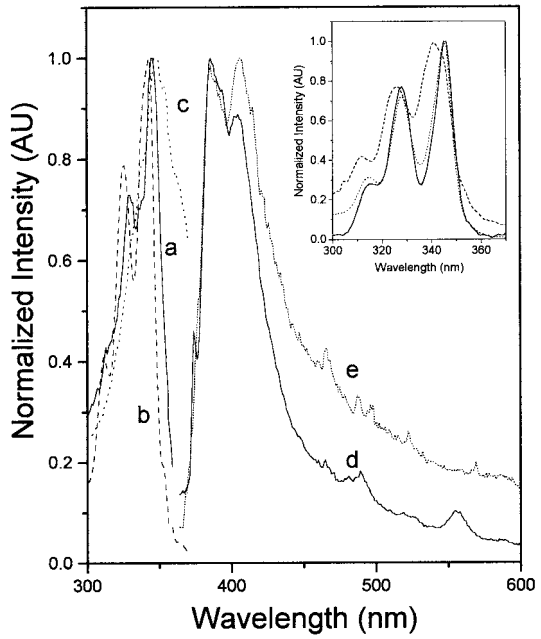

Figure 7. Normalized excitation (a, λ_{em} 374 nm; b, λ_{em} 404 nm; c, λ_{em} 485 nm) and emission (d, λ_{ex} 348 nm; e, λ_{ex} 354 nm) spectra of $\approx 5 \times 10^{-6}$ M P3P in LDPE. Inset: Normalized absorption spectra of $\approx 5 \times 10^{-6}$ M P3P in *n*-hexane (···) and LDPE (- - -); normalized excitation spectrum of $\approx 5 \times 10^{-6}$ M P3P in *n*-hexane (—, λ_{em} 373 nm).

can lead directly upon excitation to relaxed and strained excimer-like complexes.

Dynamic Fluorescence Measurements. Dynamic fluorescence rise and decay curves for the P*n*P and EtPy were recorded in PE films at 380 nm (monomer emission) and at 470 nm (when excimer-like emission was detectable). The decay constants (τ_i) and relative preexponential factors (A_i) are listed in Table 2. The monomer and excimer fluorescence response functions in PE films could be fitted satisfactorily to the sum of no more than three exponential terms (eq 1) and, in some cases, to only

$$I(t) = A_0 + A_1 e^{-t/\tau_1} + A_2 e^{-t/\tau_2} + A_3 e^{-t/\tau_3} \qquad (\tau_1 > \tau_2 > \tau_3) \tag{1}$$

two terms. One term, from scattered light ($\leq$1 ns; see Experimental Section), is not included in Table 2 or subsequent analyses. The decays from P*n*P exhibiting both monomer and excimer emissions were analyzed globally.[35]

Since the steady-state emission spectra from several of the P*n*P in PE films clearly indicate the presence of more than one distinguishable conformation, it may be only fortuitous that the decay histograms can be accommodated by no more than two exponential terms. Although the most economical fit, it may not represent fully the nature(s) of the emitting species. In fact, we initially considered a data treatment that would provide for more than one family of guest environments and would report small variations within each family via static or dynamic spectroscopic measurements. Thus, some of the rise/decay histograms were analyzed by a "distribution analysis".[36] Although mathematically satisfactory fits could be obtained for most of the individual data sets, none could be found for P3P in LDPE with λ_{em} 470 nm (i.e., the only case in which a protracted rise time was observed). In addition, the average decay constants obtained from individual samples at λ_{em} 380 and 470 nm did not appear to vary in a systematic fashion. The results from the distribution analyses of P7P in LDPE are presented as an example: at λ_{em} 380 nm ($\chi^2 = 1.225$), $\tau_1 =$

TABLE 2: Decay Constants (τ_i)[a] and Relative Preexponential Factors (A_i)[b] for $\leq 10^{-5}$ M Pyrenyl Compounds in LDPE, HDPE, and *n*-Hexane at Room Temperature ($\lambda_{ex} = 343$ nm)

guest	host	λ_{em}, nm	A_1	A_2	A_3	τ_1 (ns)	τ_2 (ns)	τ_3 (ns)	χ^2
EtPy[c]	*n*-hexane	370	1.00			201.5 ± 0.3			1.039
	HDPE	370	1.00			209.1 ± 0.3			1.199
	LDPE	370	1.00			194.0 ± 0.3			1.095
P3P	*n*-heptane[d]	376	0.047	0.052	−0.115	137.4 ± 9.9	43.1 ± 6.7	3.7 ± 1.2	1.324
		520	0.003	0.006	0.102				1.263
	LDPE	380	0.84	0.16		186.0 ± 3.6	58.9 ± 3.5		1.095
		470	1.64	−1.15					1.164
	HDPE	380	0.87	0.13		194.0 ± 4.9	68.7 ± 9.5		1.096
		470	0.54	0.46					1.104
P5P	LDPE	380	0.58	0.42		176.0 ± 6.3	45.0 ± 2.4		1.068
		470	0.35	0.65					1.001
	HDPE	380	0.95	0.05		205.8 ± 1.5	47.0 ± 4.2		1.032
		470	0.35	0.65					1.145
P7P	*n*-hexane	380	1.00			218.3 ± 0.2			1.179
	LDPE	380	0.87	0.13		203.9 ± 5.4	42.8 ± 13.4		1.085
		470	0.63	0.37					1.003
	HDPE	380	0.92	0.08		198.3 ± 3.5	50.1 ± 14.2		1.184
		470	0.60	0.40					1.013
P12P	LDPE	380	0.90	0.10		199.9 ± 7.1	62.2 ± 16.5		1.026
		470	0.60	0.40					1.177
	HDPE	380	0.95	0.05		197.5 ± 3.1	53.9 ± 6.9		1.018
		470	0.22	0.78					1.203

[a] Errors are expressed as one standard deviation. [b] A_i are expressed as relative values. [c] $\lambda_{ex} = 340$ nm. [d] $\lambda_{ex} = 344$ nm.

231.4 ± 43.3 ns (99.3%), and $\tau_2 = 12.2 \pm 1.5$ ns (0.7%); at λ_{em} 470 nm ($\chi^2 = 1.262$), $\tau_1 = 220.7 \pm 78.5$ ns (84.6%), and $\tau_2 = 77.1 \pm 12.0$ ns (15%). Since the exponential fits are excellent (as judged by χ^2 and residuals values), are more consistent internally, and lead to the conceptually simpler mechanistic models, we have invoked Ockham's razor; results from the distribution analyses are not discussed here.

The fluorescence decays from EtPy at λ_{em} 370 nm in both PE films and in *n*-hexane are monoexponential and have time constants near 200 ns. A comparable value has been obtained in *n*-heptane.[26e] In addition, the decay of emission from EtPy in LDPE at λ_{em} 470 nm was analyzed. Due to the very low emission intensity at this wavelength, there was a very large scatter spike in the first few channels. Thus, analyses were performed on data in channels after the spike; 10^4 counts were in the first channel used. The decay was fit very well to a single exponential with $\tau = 206.0 \pm 1.1$ ns ($\chi^2 = 1.078$). Although a very short decay component could have been missed, one of 40−60 ns (like that accompanying the ∼200-ns component of the P*n*P decays in the PE films; see Table 2) would not have been. On this basis, we believe that none of the very weak tail emissions at ≥450 nm from EtPy, P7P, and P12P in the PE films is from a pyrenyl complex. Decays from P7P in hexane were also found to be monoexponential, *but are biexponential in the PE films*. This result demonstrates that the biexponentiality of P*n*P decays in PE films is not a consequence of *inter*molecular interactions or impurities in the PE that interact with the probes.

As a test of our data collection and fitting routines, the fluorescence rise and decay profiles of P3P in *n*-heptane were analyzed, also. The excitation (344 nm) and emission wavelengths (376 and 520 nm) were chosen to allow comparison with the very careful work of Zachariasse et al.[26f] Despite the conditions in the two experiments being somewhat different—the temperature of the data set of Zachariasse et al. closest to ours is 60 °C and the time windows of their channels are narrower than ours—their decay constants (∼2.5, 37, and 139 ns) are very close to those found by us (3.7, 43.1, and 137.4 ns; see Table 2). A forced fit of the data to a biexponential model gave decay constants of 82.3 and 8.3 ns, but with $\chi^2 = 57.2$ (λ_{em} 376 nm) and 17.4 (λ_{em} 520 nm)! Due to the exceedingly long times required to collect 10 000 counts in the peak channel when λ_{em} was 376 nm, the background (≈320 counts/channel) was subtracted from the data and they were renormalized before being analyzed globally with the $\lambda_{em} = 520$ nm data set.

If a small amount of a short-time decay of samples such as that found for P3P in *n*-heptane were present in the PE films, it could have been masked within the channels that include the relatively large amount of scatter accompanying these histograms. However, the very large amplitude associated with the 3.7-ns component in our and others'[26f] experiments in isotropic media makes this possibility very unlikely, and a large amount of a short-time component would not have escaped detection. Similarly, the collection range employed, spanning more than 1 μs, should have permitted easy detection of a component with a longer time constant. Only in the event of a problem endemic to single-photon-counting methods, the existence of two components with similar time constants, would one have been possibly missed. Therefore, we conclude that had a mechanistically significant amount of a very different third decay component of magnitude within the time range known to be important in isotropic media been present in the PE data sets, it would have been detected.

In several samples (N.B., Figures 2, 4, and 7), steady-state measurements indicate the almost certain occurrence of static quenching (i.e., conversion of pyrenyl singlets to excimeric-like intramolecular complexes without a significant change in geometry). The consequential fluorescence rise and decay histograms must, therefore, contain rate information concerning those events. In the absence of scatter and with adequate time resolution, Webber has described how the rates can be extracted.[41] Unfortunately, the scatter channels mask whatever

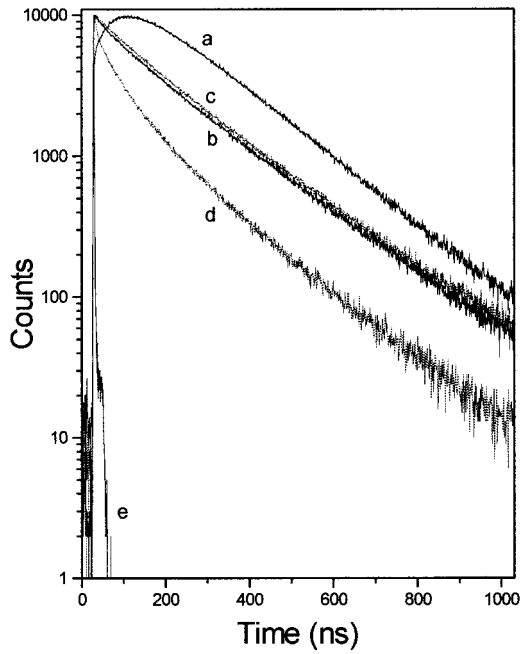

Figure 8. Time-resolved decay of emission from $\approx 5 \times 10^{-6}$ M P3P in LDPE (a, λ_{em} 470 nm; b, λ_{em} 380 nm), HDPE (c, λ_{em} 380 nm; d, λ_{em} 470 nm), and lamp profile, (e). λ_{ex} 343 nm.

information might be present and, additionally, the time scales for these events in PE are probably too short to be accessed by our equipment.

The decay curves from monomer and excimer emissions of P5P, P7P, and P12P in both PE films were fitted satisfactory to the sum of two exponential terms (Table 2), and each curve had an instrument-limited rise time. Fluorescence decay curves of P3P in HDPE and LDPE are more complex (Figure 8). The histogram from $\lambda_{em} = 470$ nm in LDPE has a slow rise component and a decay that is not monoexponential; this is the only example of a protracted rise (and a negative preexponential term that we have observed for any of the P*n*P in PE. It indicates that a large fraction, but not all, of the emission at 470 nm arises from dynamically formed excimers.[26f,42] In HDPE, the rise from the excimer component is instrument-response limited (i.e., all excimer-like emission is from excitation of preformed, ground-state conformers).

In other work, we have shown that *macroscopic* film stretching can lead to drastic *microscopic* changes in the sites occupied by guest molecule[12a,43] However, the decay constants of P3P and P7P are not altered appreciably when their LDPE or HDPE matrixes are stretched to $\sim 4\times$ their original lengths. Unfortunately, stretching led to increased light scatter and distorted decay curves that could not be analyzed fully; the preexponential factors could not be calculated precisely. Thus, although the dynamic component of excimer formation *appeared* to be absent from P3P in stretched LDPE, we cannot state definitively that it is. We conclude tentatively that occupied sites in stretched PE have smaller volumes and are more restrictive to guest motions than in unstretched PE, but do not lead to new conformations of P*n*P.

Discussion

It has been assumed by others[3,5,9,10c] and by us[12,16−18,30b] that guest molecules such as the P*n*P are unable to enter the crystalline portions of PE. Size considerations, alone, make this assumption reasonable. To test it, we examined the fluorescence of 10^{-5} M P7P (a molecule that resists intramolecular excimer formation[23,30b,44]) in *n*-heneicosane (C_{21}, a host whose crystalline lattice mimics the interior of PE crystallites[32]). At 47.5 °C (liquid phase), only monomer emission is observed. Upon being cooled rapidly to 0 °C (in an ice bath) and warming to room temperature, the solid "solution" provided an emission spectrum containing a broad band centered at ∼500 nm in addition to the still dominant monomeric fluorescence. When the liquid phase was cooled slowly to room temperature, the relative intensity of the ∼500-nm band increased by a factor of 3. By tcspc, the rise time of the emission at 500 nm is "instantaneous". These data indicate that were P*n*P molecules inside crystallites of PE, their emission would be rich in *inter*molecular excimer components. Since the spectra in PE are not, the assumption concerning the exclusion of large guest molecules from microcrystallites seems valid here.

Consequently, the *bulk* concentrations in this work are lower than those found in discrete parts of the polymer films on a microscopic scale since guests are excluded from the crystalline regions.[10c] The accessible regions of LDPE constitute ∼69% of the film, making the *average* pyrenyl concentrations ∼50% higher than that cited for the bulk; similarly, the pyrenyl concentrations in HDPE are ∼3 times the bulk values. There may be even greater intermolecular proximity since PE is known to have guest sites in specific locations of the noncrystalline parts.[10c] Regardless, the experimental evidence indicates that contact *inter*molecular processes do not contribute to the dynamic behavior of the excited states. For instance, the lack of any apparent excimeric emissions from EtPy in the PE films and the monoexponentiality of their decays demonstrate that molecular aggregation is negligible. In addition, the "corrected" concentrations are too low to expect dynamic intermolecular collisions in the very viscous[45] confines of PE: during the longest excited-state lifetimes recorded, ∼200 ns, the distance traversed by a molecule like pyrene, is calculated to be less than 1 Å.[46] Even with a gradient of concentrations within the amorphous and interfacial parts, pyrenyl containing molecules in sites separated by more than the van der Waals thickness of a methylene chain (∼3.2 Å)[47] should be unable to come into direct contact within the time frame of the excited-state measurements.

The efficiency of dipolar energy transfer over longer distances must be very low because the spectral overlap between the emission and absorption curves of a pyrenyl group is very small.[42a] The overlap that does exist can, in principle, support an inefficient long-range *radiative* energy transfer.[42] Were it an important contributor to the histograms of the P*n*P, *all* of the homologues should have exhibited "instantaneous" rise times with a superimposed protracted rise component, and the decay of EtPy in the films should not have been monoexponential. These data indicate that fluorescence decay curves from the P*n*P in PE films are a convolution of *unimolecular dynamic processes of the guests.*

Thus, the significant excimeric emissions from P3P in both PE films and from P5P in LDPE are due to *intra*molecular excited-state interactions. Moreover, since P7P has two decays ($\tau_1 \sim 200$ ns and $\tau_2 \sim 50$ ns) in both films, but only a single decay ($\tau \sim 200$ ns) in *n*-hexane, the PE must place the P*n*P in (at least) two different site types that differ only in the conformers they allow the guest to adopt (i.e., the sites are differentiable by their size and shape but not by their electrostatic nature).

The influence of the polyethylene matrixes on the *monomeric* portions of the P*n*P emission spectra is limited to a small wavelength shift caused by the polarizability of the partially aligned polymethylene chains being greater than that of hexane[38]

and, possibly, small influences of unsaturated groups along the walls of some sites and induced internal pressure (vide infra); however, in most cases, polyethylene matrixes do *not* alter the vibronic progressions of the monomeric pyrenyl emission. When intramolecular ground-state interactions are forced between pyrenyl groups by host sites, the manifestations also appear in the absorption and excitation spectra (Figures 3 and 7).

Average hole free volumes, representing the voids found in the undoped state, of nine different polyethylene samples with crystallinities varying from 31 to 80% have been determined from positron (Ps) lifetimes.[48] They (and their radii, assuming spherical cavity) are 119 Å^3 (3.1 Å) in the most crystalline and 176 Å^3 (3.5 Å) in the most amorphous sample. Since the van der Waals volume of *one* pyrenyl group is 322 Å^3,[51] the sites occupied by the P*n*P must represent a very small fraction of the total, or more likely, the occupied sites do not exist in native films but are created during the doping/swelling procedures that involve (1) swelling of the polymer by chloroform, (2) entry of P*n*P molecules into swelled sites, and (3) removal of the swelling solvent. Removal of chloroform may create additional internal pressure on the pyrenyl ring system and contribute (with polarizability effects[38]) to perturbations of the absorption and emission spectra.

The I_1/I_2 intensity ratios for P7P, P12P, and EtPy are higher in HDPE than in LDPE (Table 1). The evident complications in the emission spectra of P3P and P5P, due to the apparent coexistence of several spectroscopically distinct conformers, complicate enormously the interpretation of their I_1/I_2 ratios. For those molecules with relatively "simple" emission spectra (i.e., EtPy, P7P, and P12P), HDPE seems to enhance selectively I_1 rather than quench I_2 since the I_2/I_3 ratios (easily calculated from the data in Table 1) remain fairly constant in both PE films. The very small difference between the indices of refraction of the PE films[39] and the aforementioned factors that make bulk indices not directly applicable here make it highly unlikely that polarity is the source of the I_1/I_2 variations. Differences in *local* electronic and steric environments of different site types and/or the "internal pressure" imposed by the films[49] provide more plausible explanations. Regardless, we consider these data to be of limited interpretative value and poor diagnostics of local environments (unlike ratios from isotropic solutions[50]): (1) they are weighted averages of emissions from more than one type of host site; (2) peak *widths* in several homologues are different (making heights no longer proportional to peak *areas*, the true measure of transition probabilities); (3) the P*n*P homologues suffer varying degrees of *intra*molecular chromophore−chromophore interactions; (4) and there may be a component of complex emission buried under the structured monomer bands.

For the most part in PE, when the length of a polymethylene chain allows the pyrenyl groups of one molecule to separate themselves in a spectroscopic sense, they do so. Molecular mechanics (AM1) calculations indicate that the lengths of the P*n*P in their fully extended conformations are ∼19.5 (n = 3), 21.2 (n = 5), 24.5 (n = 7), and 31.0 Å (n = 12), and the corresponding distances between C1 atoms of the pyrenyl groups are 5.2, 7.7, 10.3, and 16.6 Å. The free volume required to accommodate *both* pyrenyl groups of a P*n*P molecule in one site (excluding the connecting chain volume) must be greater than 644 Å^3.[51] The data from P3P demonstrate that it is possible to create such sites in both LDPE and HDPE. However, data from the P*n*P with $n > 3$ show that, despite our doping conditions, even the more pliable polyethylene, LDPE, seeks to maintain sites with free volume less than 644 Å^3.[12b,c,30d] The ability of P3P to place both of its pyrenyl groups in one site (and, in some cases, to move them to an excimer conformation within the excited singlet lifetime of one lumophore) is probably a result of self-plasticization. In essence, the forced proximity of the two pyrenyl groups, due to their short tether, can disturb the dispersive interactions among the polymethylene chains that constitute the walls of the site in which they reside and lead to a reduced local viscosity.

To a certain extent, attempts to maximize van der Waals forces between the polymethylene spacer of the P*n*P with larger n and neighboring polymer chains may promote pyrenyl separation. In the interfacial regions, polymer chains must be densely packed in well-extended, parallel arrays.[1−3,5,8] However, P*n*P molecules in the amorphous regions are expected to encounter a variety of polymer chain conformations, as well as points of unsaturation and chain branching.[52] The relative disorganization afforded by sites in these regions should, therefore, allow (if not favor) P*n*P conformations that are bent (and that bring the two pyrenyl groups into an interacting proximity). Fluorescence from P*n*P in methylcyclohexane at −110 °C[23] and in PE films at room temperature display many similar features. In both cases, the conformational and translational mobility of the molecules is severely limited and the emissions occur almost exclusively from monomeric lumophores. However, in the more disorganized glassy methylcyclohexane matrix, the P*n*P can be *frozen* in the same conformations that are lowest in energy in solution since the matrix is able to adapt easily to the shapes of the guests. Although the anisotropy of local environments in PE exerts somewhat greater control over P*n*P ($n > 3$) conformations, a limited population of bent conformers, including some that may be excimer-like, appear to exist. The thermal energy available to the P*n*P (except P3P in LDPE) does not permit significant conformational changes on the time scale associated with the pyrenyl excited-state lifetimes. That "classical" excimers are not evident except with P5P in LDPE and P3P in both films suggests that *the shapes of the occupied sites are less spherical than cylindrical*.[19] In fact, the pyrenyl groups of longer P*n*P may occupy two separate sites in which their *n*-methylene chain acts as though it is a part of the matrix.

It is apparent from previous studies with a variety of organized media[12,14,16,18,19,30] that guest molecules disturb their local environments, just as the media influence the properties of the guest. The degree to which each imposes its perturbation on the other depends on a variety of factors.[17] One of these is rigidity. The rigidity of a pyrenyl group requires that the PE environment "yield" to accommodate it. When two pyrenyl groups are held near each other, especially as with P3P, PE chains in the vicinity are expected to be disturbed acutely, leading to greater fluidity. The ability of some P3P molecules to form intramolecular excimers *dynamically* in LDPE is a consequence of this disturbance; in essence, we believe that P3P residing in some PE site types is able to plasticize neighboring polymethylene chains.[53]

Why no dynamically formed excimers are evident from fluorescence histograms of P3P in HDPE and P5P in LDPE, although fluorescence spectra show clear evidence for excimer-like emissions, may be related to the specific site types available to these and the other guests. As mentioned previously, a minimum of two families of physically distinguishable sites—in the amorphous and interfacial parts—are expected in partially crystalline polyethylene.[54] In addition, perturbations caused by

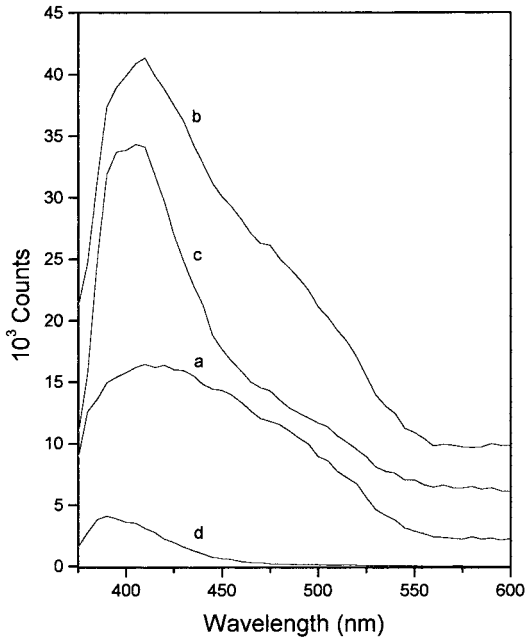

Figure 9. Time-resolved emission spectra (TRES) from ($\sim 6 \times 10^{-6}$ M) P3P in LDPE. (λ_{ex} 343 nm): (a) 4, (b) 6, (c) 8, and (d) 60 ns after excitation.

the influence of the guest molecules on their local environments, as described above, may create more.

Comparison of the magnitudes of the decay constant of EtPy with those of P7P (which is reported not to form intramolecular excimers in isotropic solvents at room temperature[23,30b]) in the PE films indicates that the families of occupied site types must be very different in size and shape. The decay constant of EtPy in PE is very similar to that of EtPy[26e] or P7P in *n*-hexane. However, *two* decay constants, as observed for P7P in HDPE or LDPE, have no analogy in isotropic media. The shorter one is consistent with the decay of an *intra*molecular, interacting species. Like P12P in both PE films and P5P in HDPE, P7P lacks an emission band that can be attributed *clearly* to a "classical" excimer. We suspect that the conformation associated with the "static" (ground-state controlled) interactions is not optimal for an excimer and that different geometries exist, depending upon the site type (vide infra). As a result, emission from the interacting lumophores is shifted to higher energy (lower wavelengths) and is largely buried under the structured, stronger emission of the monomer.

The shape of the TRES of P3P in LDPE (Figure 9) evolves from the earliest times after excitation (0−4 ns) until ∼40 ns. The emissions in the "monomer" region undergo a small hypsochromic shift during the first few nanoseconds.[55] This is consistent with those P3P molecules in sites where movement is not restricted achieving an excimer-like conformation. However, since there is a significant amount of unstructured emission at >450 nm, a relatively large fraction of the P3P exists in ground-state conformations that approximate the excimer geometry, also.

The shapes of the TRES of P3P in HDPE or P5P in both PE films (not shown) are nearly time independent; although the biexponentiality of their fluorescence decays and wavelength-dependent preexponential factors demand that the TRES change somewhat with time, the data lacked sufficient resolution to detect it visually. In part, this is due to the excimer emissions in these cases being due almost completely to excitation of conformations that approximate the complex geometries; individual histograms lack a protracted rise portion. Also, during

SCHEME 1: Simple Dynamic and Static Pathways to Emissive Species from P*n*P

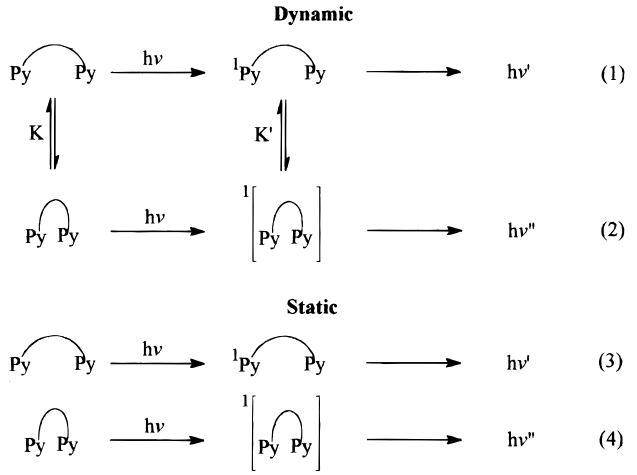

the excited-state lifetimes, there is no discernible dissociation of the excited-state complexes. The ∼200 ns decay constants found for all members of the series in both PE films (Table 2) are, thus, attributed to isolated (locally excited) pyrenyl groups that do not sense the presence of their intramolecular "partners". The ∼50 ns decay component of those P*n*P for which a classical excimer is not evident may be ascribed to conformations that allow sufficient pyrenyl−pyrenyl proximity *and orientations* (vide infra) for electronic interactions, but need *not* correspond to a relaxed excimer.

From examination of the magnitudes of the preexponential factors for the P*n*P in Table 2, combined with knowledge that the ratio of amorphous-to-interfacial volume fractions increases with the degree of PE crystallinity[18] (i.e., there are relatively fewer interfacial sites in HDPE than in LDPE), a model that associates the individual decay components with different site types can be devised. Unfortunately, it is qualitative since the partitioning of the P*n*P between the two major families of site types is also dependent upon the mode of guest introduction, the exact guest concentration, and the length of the polymethylene chain separating the two pyrenyl groups in each P*n*P homologue. However, the trends are clear: The A_1/A_2 ratios at 380 nm (for all P*n*P for which $A_1 + A_2 = 1$) are higher in HDPE than in LDPE and the ratios at 470 nm follow the opposite progression. This indicates that the P*n*P molecules associated with the τ_1 component of decay reside preferentially in the (more ordered) interfacial sites and the P*n*P molecules responsible for τ_2 are primarily in the (less ordered) amorphous sites. What remains to be discussed is the *nature* of the conformations responsible for τ_1 and τ_2.

We have presented strong evidence that some molecules of P3P in both films and P5P in LDPE are frozen in excimer-like geometries. In addition, P3P in LDPE provides a component of *dynamically* formed excimer (eqs 2 and 3 of Scheme 1). Unlike the longer P*n*P, P3P cannot dispose its pyrenyl groups so that they are well separated. In some sites provided by LDPE, but not by HDPE, the polymethylene chains constituting the walls of the cavity are made sufficiently malleable to allow conformational changes of the guests within the lifetime of a pyrenyl group in a population sufficient to be detected. For the most part, the PE results presented here can be accommodated by assuming virtually no conformational changes during the excited-state lifetimes of the P*n*P (eqs 4 and 5 of Scheme 1). The times required for changes from extended to excimeric conformations (or vice versa) are much longer than the lifetimes of the excited states.

CHART 1: Possible Conformations of a P*n*P Molecule on a Lateral Lamellar Surface of a PE Microcrystallite. the Long Axes of the Pyrenyl Groups Are at 35° with Respect to the Polymethylenic Chains (Zigzag Lines)[a] [56]

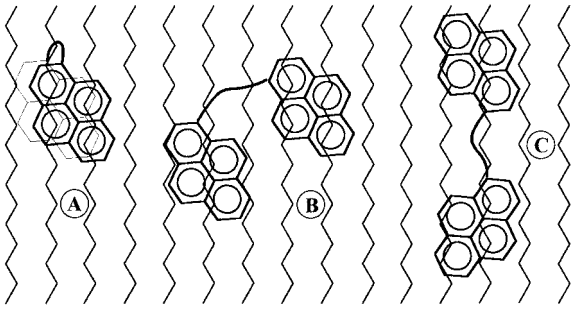

[a] (A) Sandwich (excimer) conformation; (B) long molecular axes are parallel and not overlapping; (C) long molecular axes make angle of 70° and are not overlapping.

The general species responsible for the excimeric-like emissions are represented in Chart 1 by A, two pyrenyl groups in a classical offset face-to-face orientation.[19,42] However, based upon studies of the orientation of pyrene along the lateral chains of a crystallite surface,[56] we believe that the average angle between the long molecular axes of the pyrenyl groups and neighboring extended polymethylene chains of the matrix is ~35°. In that work,[56] linear dichroic absorption measurements employing stretched (i.e., macroscopically oriented) polyethylene films and knowledge of the polarization axes of pyrene allowed the ~35° angle to be determined. A similar preferred angle should apply to the orientation of 1-alkylated pyrenyl groups in their ground or excited singlet states. Based upon this assumption, a model for the disposition of the P*n*P pyrenyl groups that accommodates the longer and shorter decay constants in PE can be devised. Equally important is the fact that *adsorption of the PnP pyrenyl groups onto a lateral surface of a PE crystallite will force them to remain in the same plane*.

The species associated with the longer of the two decay constants in PE films is easily ascribed to P*n*P excited states which lack electronic contact between the two pyrenyl groups. This separation can be achieved by spatially *or* by placing the pertinent transition dipoles at nearly orthogonal angles[57] as in Chart 1C; the emissive singlet state of pyrene is short-axis polarized[58] and that of a 1-alkylpyrene must be nearly the same. Thus, the preferred angle between pyrenyl groups of this sort is ~70°and so is the angle between their transition dipoles. The excited states of molecules whose pyrenyl groups are represented by Chart 1C are expected to behave like EtPy.

We tentatively attribute the species responsible for the shorter decay constant to P*n*P singlets in which the individual pyrenyl groups are disposed at angles (*and distances*) that are expected to provide strong pyrenyl−pyrenyl excitation dipole interactions as in Chart 1B, where the long molecular axes *and* transition dipoles of the pyrenyl groups are nearly parallel. Conformations of P*n*P like those in Chart 1B, "frozen" along a lateral face, allow the pyrenyl groups to be at the preferred pyrene angle and the chain between them to lie approximately in phase with the crystallite polymethylene lamellae.[59] *The conformations given in Chart 1B and C represent a negligible fraction of the total population in solution or in frozen isotropic matrixes, but can dominate in a medium like PE*. Obviously, more experimentation will be required to determine whether our model is correct. If it is, PE will offer an easy method to investigate interchromophoric interactions in very specific molecular orientations that cannot be achieved in other media, including very anisotropic ones.

Acknowledgment. We thank the Petroleum Research Fund (administered by the American Chemical Society) and the National Science Foundation for their support of this work. The reviewers and Prof. Frank Quina are also thanked for several interesting suggestions.

References and Notes

(1) Bovey, F. A. *Chain Structure and Conformation of Macromolecules*; Academic Press: New York, 1982.

(2) (a) Till, P. H. *J. Polym. Sci.* **1957**, *24*, 301. (b) Keller, A. *Philos. Mag.* **1957**, *2*, 1171. (c) Fisher, E. W. *Z. Naturforsch.* **1957**, *12A*, 753.

(3) Peterlin, A. *Macromolecules* **1980**, *13*, 777.

(4) Clark, E. S. *Polymeric Materials*; American Society for Metals: Metals Park, OH, 1974; Chapter 1.

(5) Wunderlich, B. *Macromolecular Physics*; Academic Press: New York, 1974; Vol. I.

(6) Strobl, G. R.; Hagerdon, W. *J. Polym. Sci., Polym. Phys. Ed.* **1978**, *16*, 1181.

(7) Zielinski, J. M.; Duda, J. L. *AIChE J.* **1992**, *38*, 405.

(8) Elias, H. *Macromolecules I, Structure and Properties*; Plenum Press: New York. 1984; p 185.

(9) Vieth, W. R. *Diffusion In and Through Polymers*; Hanser Verlag: Munich, 1991.

(10) (a) Thulstrup, E. W.; Eggers, J. H. *Chem. Rev. Lett.* **1968**, *1*, 690. (b) Thulstrup, E. W.; Michl, J.; Eggers, J. H. *J. Phys. Chem.* **1970**, *74*, 3868. (c) Phillips, P. J. *Chem. Rev.* **1990**, *90*, 425 and references therein.

(11) Thulstrup, E. W.; Michl, J. *Elementary Polarization Spectroscopy*; VHS: New York, 1989; Chapter 2.

(12) (a) Ramesh, V.; Weiss, R. *Macromolecules* **1986**, *19*, 1489. (b) Naciri, J.; Weiss; R. G. *Macromolecules* **1989**, *22*, 3928. (c) Jenkins, R. M.; Hammond, G. S.; Weiss, R. G. *J. Phys. Chem.* **1992**, *96*, 496. (d) Cui, C. X.;; Weiss, R. G. *J. Am. Chem. Soc.* **1993**, *115*, 9820.

(13) (a) Wittmann, J. C.; Lotz, B. *J. Polym. Sci., Polym. Phys. Ed.* **1981**, *19*, 1837. (b) Wittmann, J. C.; Hodge, A. M.; Lotz, B. *J. Polym. Sci., Polym. Phys. Ed*. **1983**, *21*, 2495.

(14) (a) Szadkowska-Nicze, M.; Mayer, J.; Kroh, J. *J. Photochem. Photobiol. A: Chem.* **1990**, *54*, 389. (b) Johnson, G. E. *Macromolecules* **1980**, *13*, 839.

(15) For an excellent review, see: Thulstrup, E. W.; Michl, J. *Spectrochim. Acta* **1988**, *44A*, 767.

(16) (a) He, Z.; Hammond, G. S.; Weiss, R. G. *Macromolecules* **1992**, *25*, 1568. (b) Lu, L.; Weiss, R. G. *Macromolecules* **1994**, *27*, 219.

(17) Weiss, R. G.; Ramamurthy, V.; Hammond, G. S. *Acc. Chem. Res.* **1993**, *26*, 530.

(18) Zimerman, O. E.; Cui, C. X.; Wang; X.; Atvars, T. D. Z.; Weiss. R. G. *Polymer* **1998**, *39*, 1177.

(19) (a) Cui, C.; Naciri, J.; Hé, Z.; Jenkins, R. M., Lu, L.; Ramesh, V.; Hammond, G. S.; Weiss; R. G. *Quím. Nova* **1993**, *16*, 578. (b) See ref 17 and references therein.

(20) Szadkowska-Nicze, M.; Wolszczak, M.; Kroh, J.; Mayer, J. *J. Photochem. Photobiol. A: Chem.* **1993**, *75*, 125.

(21) Avis, P.; Porter, G. *J. Chem Soc.* **1973**, *34*, 1057.

(22) Itaya, A.; Kurahashi, A.; Masuhara, H.; Taniguchi, Y.; Kiguchi, M. *J. Appl. Phys.* **1990**, *67*, 2240.

(23) Zachariasse, K. A.; Kühnle, W. *Z. Phys. Chem. Neue Folge.* **1976**, *101*, 267.

(24) See, for instance: (a) de Schryver, F. C.; Collart, P.; Vandendriessche, J.; Goedeweeck, R.; Swinnen, A.; Van der Auweraer, M. *Acc. Chem. Res.* **1987**, *20*, 159. (b) Reynders, P.; Kühnle, W.; Zachariasse, K. A. *J. Phys. Chem.* **1990**, *94*, 4073.

(25) Hara, K.; Yano, H. *J. Am. Chem. Soc.* **1988**, *110*, 1911.

(26) (a) Snare, M. J.; Thisttlethwaite, P. J.; Ghiggino, K. P. *J. Am. Chem. Soc.* **1983**, *105*, 3328. (b) Zachariasse, K. A.; Duveneck, G.; Busse, R. *J. Am. Chem. Soc.* **1984**, *106*, 1045. (c) Zachariasse, K. A.; Busse, R.; Duveneck, G.; Kühnle, W. *J. Photochem.* **1985**, *28*, 237. (d) Siemiarczuk, A.; Ware, W. R. *Chem. Phys. Lett.* **1987**, *140*, 277. (e) Zachariasse, K. A.; Striker, G. *Chem. Phys. Lett.* **1988**, *145*, 251. (f) Zachariasse, K. A.; Kühnle, W.; Leinhos, U.; Reynders, P.; Striker, G. *J. Phys. Chem.* **1991**, *95*, 5476.

(27) Although the work presented here does not bear directly on that controversy, we favor the model proposed by Zachariasse et al.[26f]

(28) Kano, K.; Ishibashi, T.; Ogawa, T. *J. Phys. Chem.* **1983**, *87*, 3010.

(29) Zachariasse, K. A.; Kühnle, W.; Weller, A. *Chem. Phys. Lett.* **1980**, *73*, 6.

(30) (a) Sonnenchein, M. F.; Weiss, R. G. In *Photochemistry on Solid Surfaces*; Matsuura, T., Anpo, M., Eds.; Elsevier: Amsterdam, 1981; p 526. (b) Anderson, V. C.; Weiss, R. G. *J. Am. Chem. Soc.* **1984**, *106*, 5291. (c) Sonnenchein, M. F.; Weiss, R. G. *J. Phys. Chem.* **1988**, *92*, 6828. (d) Jenkins, R. M.; Weiss, R. G. *Langmuir* **1990**, *6*, 1408.

(31) Josephy, E., Radt, F., Eds. *Elsevier's Encyclopedia of Organic Chemistry*; Elsevier: New York, 1940; Series III, Vol. 14, p 379.

(32) Sirota, E. B.; Singer, D. M. *J. Chem. Phys.* **1994**, *101*, 10873.

(33) Graselli, J. G.; Ritchey, W. M. *Atlas of Spectral Data and Physical Constants for Organic Compounds*, 2nd ed.; CRC Press: Cleveland, OH, 1975; Vol. IV, p 369.

(34) For P7P and P12P in HDPE at λ_{em} 470 nm, the histograms exhibited a spike due to scattered light. In those cases, $\sim 10^4$ counts were collected in the channel immediately after the spike and data analysis excluded the first few channels.

(35) (a) Eaton, D. F. *Pure Appl. Chem.* **1990**, *62*, 1631 and references therein. (b) Knutson, J. R.; Beechem, J. M.; Brand, L. *Chem. Phys. Lett.* **1983**, *102*, 501. (c) Beechem, J. M.; Ameloot, M.; Brand, L. *Chem. Phys. Lett.* **1985**, *120*, 466.

(36) (a) Liu, Y. S.; Ware, W. R. *J. Phys. Chem.* **1993**, *97*, 5980. (b) Liu, Y. S.; de Mayo, P.; Ware, W. R. *J. Phys. Chem.* **1993**, *97*, 5987. (c) Liu, Y. S.; de Mayo, P.; Ware, W. R. *J. Phys. Chem.* **1993**, *97*, 5995.

(37) λ_{ex} 354 nm yielded TRES spectra in which signal/noise was very low.

(38) (a) Boyd, R. H.; Kesner, L. *Macromolecules* **1987**, *20*, 1802. (b) Lamotte, M.; Joussot-Dubien, J. *Chem. Phys.* **1973**, *2*, 245. (c) Lamotte, M.; Joussot-Dubien, J.; Mantione, M. J.; Claverie, P. *Chem. Phys. Lett.* **1974**, *27*, 515.

(39) Seferis, J. C. In *Polymer Handbook*, 3rd ed.; Brandrup, J., Immergut, E. H., Eds.; Wiley: New York, 1989; p VI/459.

(40) Sakamoto, K.; Yoshida, R.; Hatano, M.; Tachibana, T. *J. Am. Chem. Soc.* **1978**, *100*, 6898.

(41) Webber, S. E. *Photochem. Photobiol.* **1997**, *65*, 33.

(42) (a) Birks, J. B. *Photophysics of Aromatics Molecules*; Wiley: London, 1970; p 301. (b) Barltrop, J. A.; Coyle, J. D. *Principles of Photochemistry*; Wiley: Bristol, U.K., 1975; p 105.

(43) (a) Cui, C.; Weiss, R. G. *J. Am. Chem. Soc.* **1993**, *115*, 9820. (b) Wang, X.; Gu, W.; Bhattacharjee, U.; Weiss, R. G., unpublished results.

(44) Zachariasse, K. A.; Duveneck, G.; Kühnle, W.; Leinhos, U.; Reynders, P. In *Photochemical Processes in Organized Molecular Systems*; Honda, K., Ed.; Elsevier: Amsterdam, 1990; p 83.

(45) Rodriguez, F. *Principle of Polymer Systems*; Taylor & Francis: London, 1996; Chapter 7.

(46) The diffusion coefficient D of 4.7×10^{-12} cm^2/s in poly(isobutyl methacrylate) (near the glass transition temperature (25 °C)) is assumed. Deppe, D. D.; Miller, R. D.; Torlkelson, J. M. *J. Polym. Sci., Polym. Phys. Ed.* **1996**, *34*, 2987.

(47) Bondi, A. *J. Phys. Chem.* **1964**, *68*, 441.

(48) Serna, J.; Abbé, J. Ch.; Duplâtre, G. *Phys. Status Solidi A* **1989**, *115*, 389.

(49) (a) Ferry, J. D. *Viscoelastic Properties of Polymers*; Wiley: New York, 1970; Chapter 11. (b) Matheson, A. J. *J. Chem. Phys.* **1962**, *44*, 695.

(50) (a) Kalyanasundaram, K.; Thomas, J. K. *J. Am. Chem. Soc.* **1977**, *99*, 2039. (b) Kalyanasundaram, K.; Thomas, J. K. *J. Phys. Chem.* **1977**, *81*, 2176. (c) Dong, D. C.; Winnik, M. A. *Photochem. Phobiol.* **1982**, *35*, 17.

(51) Cameron, A.; Trotter, J. *Acta Crystallogr.* **1965**, *18*, 636.

(52) The degree of branching can be inferred from the frequency of methyl groups.[18]

(53) Mark, J. E.; Eisenberg, A.; Graessley, W. W.; Mandelkern, L.; Samulski, E. T.; Koening, J. L.; Wignall, G. D. *Physical Properties of Polymers*, 2nd ed.; American Chemical Society: Washington, DC, 1993; pp 83−85.

(54) A third interfacial region (and even a forth, disordered but anisotropic component) has been suggested: Mutter, R.; Sitle, W.; Strobl, G. R. *J. Polym. Sci., Polym. Phys. Ed.* **1993**, *31*, 99.

(55) Since the TRES are an unweighted sum of data from 10 channels contiguous in time and the longer wavelength portions (e.g., 470 nm), especially, have fewer data points than the shorter wavelength portions, no direct comparison of the decays of intensity should be made between Figures 8 and 9. The TRES intensities, as plotted in Figure 8, are smoothed and provide only an approximation of the temporal events; the data sets in Figure 9 contain many more counts at 470 nm and represent the best assessment of the dynamic changes.

(56) Konwerska-Hrabowska, J. *Appl. Spectrosc.* **1985**, *39*, 434.

(57) See, for instance: Kasha, M.; Rawls, H. R.; El-Bayoumi, M. *Pure Appl. Chem.* **1965**, *11*, 371.

(58) (a) Langkilde, F. W.; Gisin, M.; Thulstrup, E. W.; Michl, J. *J. Phys. Chem.* **1983**, *87*, 2901. (b) Langkilde, F. W.; Thulstrup, E. W.; Michl, J. *J. Chem. Phys.* **1983**, *78*, 3372.

(59) We are currently performing calculations (based upon previous results[56]) to determine whether the conformations in Chart 1 represent energy minima for α,ω-di(1-pyrenyl)alkanes as they lie along the lateral surfaces of a crystallite.